ChemComm

COMMUNICATION

View Article Online
View Journal | View Issue

A highly selective water-soluble optical probe for endogenous peroxynitrite†

Ji-Ting Hou,[a] Jin Yang,[a] Kun Li,*[ab] Ye-Xin Liao,[a] Kang-Kang Yu,[a] Yong-Mei Xie[b] and Xiao-Qi Yu*[a]

Cite this: *Chem. Commun.*, 2014, **50**, 9947

Received 2nd June 2014,
Accepted 11th July 2014

DOI: 10.1039/c4cc04192e

www.rsc.org/chemcomm

A colorimetric and fluorescent probe C-Py-1 for $ONOO^-$ was prepared and it could exhibit high sensitivity and excellent selectivity toward $ONOO^-$ among reactive oxygen species (ROS) and reactive nitrogen species (RNS) with a rapid response time in 100% water solution. Meanwhile, C-Py-1 was successfully applied in the imaging of endogenous $ONOO^-$ in RAW264.7 cells.

Peroxynitrite ($ONOO^-$) acts as a highly reactive oxidant *in vivo*, which is formed through a diffusion-controlled reaction between nitric oxide (NO) and superoxide ($O_2^{\bullet -}$) in a 1 : 1 stoichiometry (k = 0.4–1.9 × 10^{10} M^{-1} s^{-1}).[1] Compared with the acid form (ONOOH), peroxynitrite is relatively stable with a half-life of ~1 s at pH 7.4,[2] and it can damage a wide array of molecular components in cells, including DNA and proteins, owing to its high oxidizing and nitrating potential.[3] Nevertheless, an abnormal peroxynitrite level can contribute to pathogenic effects, such as cardiovascular, neurodegenerative, inflammatory diseases and diabetes.[4]

Comprehending the vital role peroxynitrite plays in the biosystem, the development of sensitive and selective techniques for detecting peroxynitrite is fairly valuable and meaningful.[5] Until now, several approaches have been developed for the detection of peroxynitrite, including UV/Vis spectroscopy, electrochemical analysis, electron spin resonance, and immunohistochemistry.[6] However, the precise pathogenic role of peroxynitrite in biological systems is still not very clear due to the short life-time, high activity, low concentration, and elusive nature of peroxynitrite *in vivo*. By contrast, fluorimetry for peroxynitrite detection has been developed in the past few decades due to its high measurement efficiency, non-invasive detection and excellent spatial and temporal resolution.[7]

To date, a number of fluorescent peroxynitrite sensors have been reported and applied to the *in vitro* and *in vivo* imaging of peroxynitrite,[8,9] which further promoted the study of the behavior of peroxynitrite in biological processes. However, some problems of these probes might be encountered, such as interference from other highly reactive oxidants (especially from ClO^- and $^{\bullet}OH$), low quantum yield and small Stokes shift (<20 nm). Especially, only a few reported probes could detect endogenous peroxynitrite.[9] Thus, developing novel effective fluorescent probes for detecting endogenous peroxynitrite is in an urgent demand. Herein, we report two compounds **C-Py-1** and **C-Py-2** based on a coumarin platform and explore their optical response toward reactive oxygen species (ROS) and reactive nitrogen species (RNS). The coumarin scaffold is chosen as the fluorophore owing to its good photostability, large Stokes shift and high quantum yield,[10] and the pyridinium moiety was introduced to increase the water solubility. Interestingly, **C-Py-1** was found to selectively detect peroxynitrite in 100% PBS (pH 7.4, 10 mM), while **C-Py-2** remained almost unchanged in the presence of various reactive species, implying that the substituent on the 7-position of coumarin displayed a profound influence on the reactivity of the probe. These two compounds were prepared *via* a simple process and characterized by ^1H, ^{13}C NMR and HRMS (see ESI†) (Scheme 1).

Initially, to evaluate whether **C-Py-1** or **C-Py-2** can exhibit optical response toward ROS and RNS, we measured the absorption and emission spectra of these two compounds in the presence of various ROS and RNS. To the solution of 5 μM **C-Py-1** in PBS (pH 7.4, 10 mM) was added 50 μM $ONOO^-$ and the absorption peak at 514 nm (ε_{514nm} = 35 100 M^{-1} cm^{-1}) was reduced and

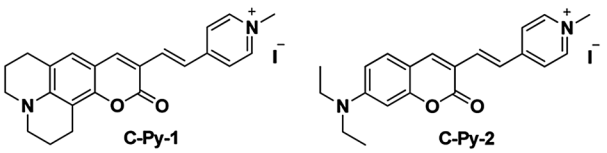

Scheme 1 The structures of **C-Py-1** and **C-Py-2**.

[a] *Key Laboratory of Green Chemistry and Technology, Ministry of Education, College of Chemistry, Sichuan University, Chengdu, 610064, P. R. China. E-mail: kli@scu.edu.cn, xqyu@scu.edu.cn; Fax: +86-28-85415886*
[b] *State Key Laboratory of Biotherapy, West China Hospital, West China Medical School, Sichuan University, Chengdu 610041, China*

† Electronic supplementary information (ESI) available: Synthesis of the probes and intermediates, as well as their spectra. See DOI: 10.1039/c4cc04192e

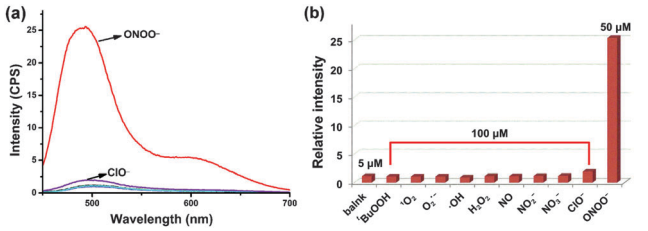

Fig. 1 (a) Fluorescence spectra and (b) fluorescence intensity of **C-Py-1** at 493 nm before and after reaction with various ROS and RNS in PBS (pH 7.4, 10 mM). [**C-Py-1**] = 5 μM. $ONOO^-$: $ONOO^-$ (final 50 μM) was added and the mixture was stirred at 20 °C. ClO^-: NaClO (final 100 μM) was added and the mixture was stirred at 20 °C. •OH: ferrous perchlorate (100 μM) and H_2O_2 (0.2 mM) were added at room temperature. $O_2^{\bullet-}$: KO_2 was dissolved in the anhydrous DMSO and then the appropriate aliquot was added (final 100 μM). H_2O_2: H_2O_2 (final 100 μM) was added and the mixture was stirred at 20 °C. ^{t}BuOOH: ^{t}BuOOH (final 100 μM) was added and the mixture was stirred at 20 °C. $^1O_2$: ClO^- (100 μM) and H_2O_2 (0.2 mM) were added at room temperature; NO: NOC-5 (a NO donor) was added and the mixture was stirred at 20 °C (final 100 μM). NO_2^-: $NaNO_2$ (final 100 μM) was added and the mixture was stirred at 20 °C. NO_3^-: $NaNO_3$ (final 100 μM) was added and the mixture was stirred at 20 °C. λ_{ex} = 425 nm, slit: 3 nm/3 nm.

blue-shifted to 484 nm, accompanied by a colour change from pink to light yellow (Fig. S1, ESI†). When 100 μM other ROS and RNS (*i.e.* •OH, $O_2^{\bullet-}$, H_2O_2, ClO^-, ^{t}BuOOH, $^1O_2$, NO) were added to the solution of **C-Py-1**, only an inconspicuous decrement of the absorption peak of **C-Py-1** was observed. Additionally, the addition of 100 μM common nitrogen-containing anions, NO_2^- and NO_3^-, did not influence the absorption profiles of **C-Py-1**. On the other hand, with the addition of tested species to the solution of 5 μM **C-Py-2** in PBS (pH 7.4, 10 mM), almost no changes in the absorption peak at 491 nm were observed except that the addition of $ONOO^-$ caused a little decrement. Simultaneously, the addition of $ONOO^-$ to the solution of **C-Py-1** also induced a 25-fold fluorescence enhancement at 493 nm, as shown in Fig. 1. However, the addition of other species caused negligible variation of the fluorescence intensity. As for **C-Py-2**, the addition of various species including $ONOO^-$ could not change its emission spectra, indicating that the activity of **C-Py-2** might be lower than that of **C-Py-1** (Fig. S2, ESI†). Indeed, the oxidation potential of **C-Py-1** measured by cyclic voltammetry was lower than that of **C-Py-2**, 0.178 V for **C-Py-1** and 0.289 V for **C-Py-2**, respectively (Fig. S3, ESI†). Since a dye whose oxidation potential was lower displayed higher ROS reactivity,[8e] the cyclic voltammetry experiment results agreed with the optical measurements that **C-Py-1** was more reactive than **C-Py-2**. We ascribed this higher reactivity to the richer electron density of **C-Py-1** with a stronger electron-donating group.

Considering that the carbon–carbon double bond and the pyridinium salt moiety of **C-Py-1** might react with some nucleophiles like SO_3^{2-} and Cys, the fluorescence responses of **C-Py-1** toward different kinds of nucleophilic agents were tested. When 100 μM SO_3^{2-}, S^{2-}, F^-, CN^-, GSH, Cys or Hcy were added to the solution of 5 μM **C-Py-1** in PBS, only S^{2-} and Cys could induce a 2–3 fold fluorescence enhancement at 493 nm, suggesting that **C-Py-1** was fairly stable in the presence of various nucleophiles (Fig. S4, ESI†). Accordingly, **C-Py-1** could act as a highly selective and sensitive probe for $ONOO^-$ in water.

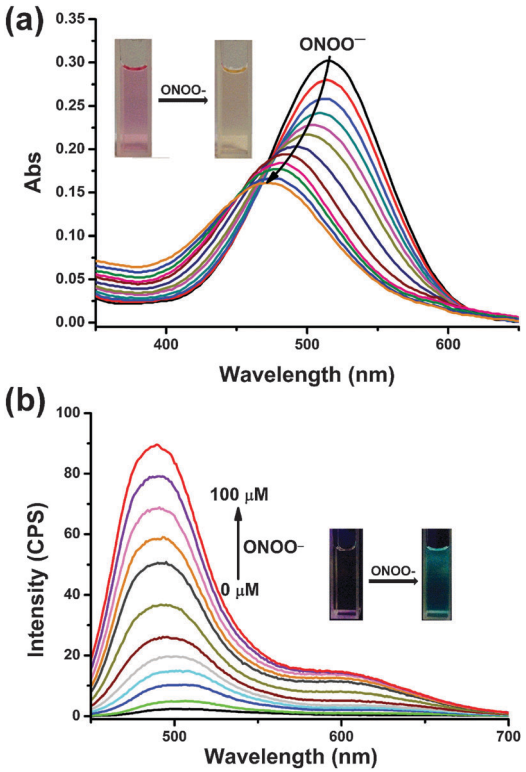

Fig. 2 (a) UV-vis and (b) fluorescence titration spectra of **C-Py-1** upon the addition of $ONOO^-$ (0, 2, 5, 10, 15, 20, 30, 40, 50, 60, 80, 100 μM) in PBS (pH 7.4, 10 mM). [**C-Py-1**] = 5 μM, λ_{ex} = 425 nm, slit: 3 nm/3 nm. Inset: the colour change of **C-Py-1** before and after the addition of $ONOO^-$: (a) under daylight and (b) under UV lamp (ex = 365 nm).

Then, the titration experiments of **C-Py-1** toward $ONOO^-$ were explored. As depicted in Fig. 2, **C-Py-1** in PBS displayed a unique absorption peak at 514 nm, attributed to the strong intramolecular charge transfer from the amino group to the pyridinium moiety. Upon the addition of $ONOO^-$ (0–100 μM), the absorption intensity was reduced and a hypochromatic shift of 44 nm as well as a colour change from pink to light yellow was observed. Fluorescence titration experiments also showed that the fluorescence of **C-Py-1** at 493 nm could be enhanced apparently upon addition of $ONOO^-$, and a linearly proportional increment of emission intensity to the concentration of $ONOO^-$ in the range of 0–20 μM was disclosed (Fig. S5, ESI†). In fact, **C-Py-1** displayed a quite weak emission at 652 nm in PBS with a Stokes shift of 138 nm when excited at 514 nm, and the quenching of fluorescence might be caused *via* the formation of a hydrogen bond between **C-Py-1** and H_2O (Fig. S6, ESI†).[11] According to the titration profiles, the detection limit (S/N = 3) of **C-Py-1** toward $ONOO^-$ was calculated to be 1.5×10^{-7} M. The quantum yield of **C-Py-1** was as low as 0.012 and reached 0.26 in the presence of $ONOO^-$. The effect of pH on the fluorescence response of **C-Py-1** toward $ONOO^-$ was also investigated (Fig. S7, ESI†). The results showed that $ONOO^-$ could induce a significant emission amplification of **C-Py-1** in a pH range from 6 to 9, indicating that **C-Py-1** could detect $ONOO^-$ under physiological conditions.

Subsequently, the reaction dynamics between **C-Py-1** and $ONOO^-$ was measured (Fig. S8, ESI†). **C-Py-1** was non-emissive

before the addition of $ONOO^-$ and the fluorescence of **C-Py-1** remained extremely steady even for an hour. However, the emission intensity of **C-Py-1** increased profoundly and reached a plateau in 4 minutes once 5 equiv. $ONOO^-$ was added, and a slow increment was observed in the further tens of minutes, indicating that the reaction between **C-Py-1** and $ONOO^-$ could be basically accomplished within a few minutes.

Recently, Nagano's group has reported that the polymethine chain of Cy7 could be cleaved to afford 1,3,3-trimethyloxindole in the presence of ROS (including $ONOO^-$).[8e] Thus, we suspected that the carbon–carbon double bond of **C-Py-1** might be cleaved upon the oxidation of $ONOO^-$ and a fluorescent product was simultaneously generated. To confirm our assumption, the reaction solution of **C-Py-1** and $ONOO^-$ underwent the ESI-MS analysis (Fig. S9, ESI†). The prominent peak at *m*/*z* 270.1129 corresponding to aldehyde **4** (the *m*/*z* of $[\mathbf{4}+H]^+$ was calculated to be 270.1130) was found in MS spectra, implying the production of aldehyde **4**. Meanwhile, the UV-vis absorption and fluorescence spectra of **4** in PBS were monitored. The absorption maximum and emission peaks appeared at 464 nm (ε_{464nm} = 49 000 M^{-1} cm^{-1}) and 510 nm (the Stokes shift is 46 nm), respectively (Fig. S10, ESI†), which are quite close to that of **C-Py-1** in the presence of $ONOO^-$. Some small deviation could be attributed to the complicated reaction environment. The shoulder peak at around 620 nm for **C-Py-1** in the presence of $ONOO^-$ might be ascribed to the reaction intermediates.[12] To further confirm the reaction mechanism, we finally conducted the ^1H NMR analysis of the mixture of **C-Py-1** and $ONOO^-$. When $ONOO^-$ was added into the solution of **C-Py-1** in DMSO-d_6, a typical signal peak at 9.88 ppm was observed, which apparently indicated the formation of the aldehyde group (Fig. S11, ESI†). Thus, aldehyde **4** might be the primary product in the reaction of **C-Py-1** and $ONOO^-$, as depicted in Scheme 2.

The desirable fluorescence properties of **C-Py-1** for $ONOO^-$ prompted us to use it for the detection of intracellular $ONOO^-$. A standard MTT assay showed that cell viability was rarely changed even though 20 μM **C-Py-1** was added for 24 h (Fig. S12, ESI†), signifying the extremely low cytotoxicity of **C-Py-1**. Then, confocal microscopy experiments were carried out on RAW264.7 cells. RAW264.7 cells were incubated with 10 μM **C-Py-1** for 30 min at 37 °C in DMEM. Upon excitation at 405 nm, there was no intracellular blue fluorescence between 450–520 nm, as shown in Fig. 3. When 50 μM 3-morpholinosydnonimine (SIN-1, a $ONOO^-$ donor) was added and was then incubated for another 60 min, apparent fluorescence emerged in the cytoplasm of **C-Py-1**-loaded cells, showing that **C-Py-1** permeates cells well and can detect intracellular $ONOO^-$.

Inspired by the above biological experimental results, we would like to utilize **C-Py-1** to sense endogenous $ONOO^-$ in RAW264.7 cells, which are known to generate ROS and RNS in

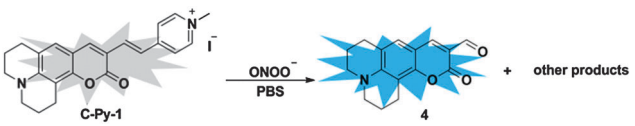

Scheme 2 The proposed reaction of **C-Py-1** with $ONOO^-$.

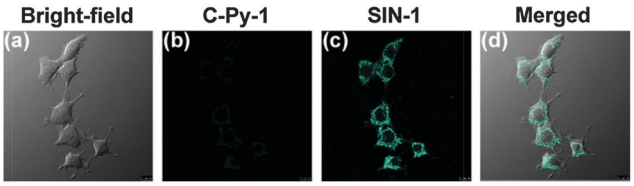

Fig. 3 Confocal fluorescence images of RAW 264.7 cells. (a) Bright-field image; (b) cells were stained with **C-Py-1** (10 μM) for 30 min, (c) and then incubated with SIN-1 (50 μM) for 60 min; (d) merged image of (a) and (c) scale bars: 10 μm.

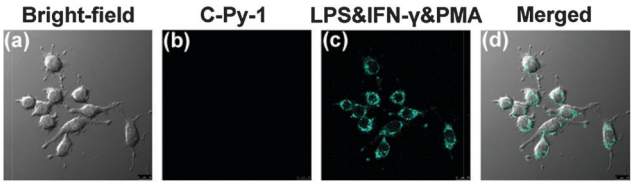

Fig. 4 Confocal fluorescence images of RAW 264.7 cells. (a) Bright-field image; (b) cells were stained with **C-Py-1** (10 μM) for 30 min; (c) cells were stained with LPS (1 μg mL^{-1}) and IFN-γ (50 ng mL^{-1}) for 4 h and were then incubated with PMA (10 μg mL^{-1}) for 0.5 h and were incubated with **C-Py-1** (10 μM) for 0.5 h; (d) merged image of (a) and (c) scale bars: 10 μm.

immunological and inflammatory processes.[13] RAW 264.7 cells were first treated with lipopolysaccharide (LPS, 1 μg mL^{-1}) and interferon-γ (IFN-γ, 50 ng mL^{-1}) for 4 h and were then incubated with phorbol 12-myristate 13-acetate (PMA, 10 μg mL^{-1}) for another 0.5 h. Finally, 10 μM **C-Py-1** was added and stained for 30 min. As shown in Fig. 4(c), obvious fluorescence appeared in RAW264.7 cells stimulated with different reagents and **C-Py-1**. However, no fluorescence was observed in **C-Py-1**-loaded cells (Fig. 4(b)). This result indicated that **C-Py-1** was successfully applied in detecting endogenous $ONOO^-$ in RAW264.7 cells, which is of considerable significance for an effective small molecular fluorescent probe having biological applications.

In conclusion, two coumarin–pyridinium conjugates **C-Py-1** and **C-Py-2** were synthesized while only **C-Py-1** showed colorimetric and fluorescent responses toward $ONOO^-$, which might be due to the much richer electron density of **C-Py-1** with a stronger electron-donating group. **C-Py-1** exhibited high sensitivity and excellent selectivity toward $ONOO^-$ among ROS and RNS with a rapid response time, while other nucleophilic anions showed no interference. The reaction mechanism was suspected to be the oxidative cleavage of the carbon–carbon double bond of **C-Py-1** *via* ESI-MS analysis and UV spectra study. Ultimately, **C-Py-1** was successfully applied in the imaging of endogenous $ONOO^-$ in RAW264.7 cells with outstanding cell membrane penetrability and low cytotoxicity. We anticipate that **C-Py-1** can be utilized in a variety of chemical and biological applications owing to its easy preparation and excellent chemical and biological properties, and this work is expected to provide some valuable exploration for the strategical design of peroxynitrite-targeted fluorescent probes.

This work was financially supported by the National Program on Key Basic Research Project of China (973 Program, 2012CB720603 and 2013CB328900), the National Science Foundation of

China (No. 21232005, 21321061, J1310008 and J1103315), and the Specialized Research Fund for the Doctoral Program of Higher Education in China (20120181130006).

Notes and references

1 (*a*) C. Szabo, H. Ischiropoulos and R. Radi, *Nat. Rev. Drug Discovery*, 2007, **6**, 662–680; (*b*) F. C. Fang, *Nat. Rev. Microbiol.*, 2004, **2**, 820–832; (*c*) G. L. Squadrito and W. A. Pryor, *Free Radical Biol. Med.*, 1998, **25**, 392–403; (*d*) J. S. Beckman, T. W. Beckman, J. Chen, P. A. Marshall and B. A. Freeman, *Proc. Natl. Acad. Sci. U. S. A.*, 1990, **87**, 1620–1624.

2 N. Ashki, K. C. Hayes and F. Bao, *Neuroscience*, 2008, **156**, 107–117.

3 (*a*) H. Kaur and B. Halliwell, *FEBS Lett.*, 1994, **350**, 9–12; (*b*) R. T. Dean, S. Fu, R. Stocker and M. J. Davies, *Biochem. J.*, 1997, **324**, 1–18.

4 (*a*) J. S. Beckman, M. Carson, C. D. Smith and W. H. Koppenol, *Nature*, 1993, **364**, 584–585; (*b*) H. Wiseman and B. Halliwell, *Biochem. J.*, 1996, **313**, 17–29; (*c*) S. M. Schieke, K. Briviba, L. O. Klotz and H. Sies, *FEBS Lett.*, 1999, **448**, 301–303; (*d*) W. Kossenjans, A. Eis, R. Sahay, D. Brochman and L. Myatt, *Am. J. Physiol.: Heart Circ. Physiol.*, 2000, **278**, 1311–1319; (*e*) P. Pacher, J. S. Beckman and L. Liaudet, *Physiol. Rev.*, 2007, **87**, 315–424.

5 (*a*) T. Nagano, *J. Clin. Biochem. Nutr.*, 2009, **45**, 111–124; (*b*) G. Ferrer-Sueta and R. Radi, *ACS Chem. Biol.*, 2009, **4**, 161–177.

6 (*a*) A. Vandervliet, J. P. Eiserich, C. A. Oneill, B. Halliwell and C. E. Cross, *Arch. Biochem. Biophys.*, 1995, **319**, 341–349; (*b*) K. Dai, A. G. Vlessidis and N. P. Evmiridis, *Talanta*, 2003, **59**, 55–65; (*c*) S. B. Digerness, K. D. Harris and J. W. Kirklin, *Free Radical Biol. Med.*, 1999, **27**, 1386–1392; (*d*) S. F. Peteu, R. Boukherroub and S. Szunerits, *Biosens. Bioelectron.*, 2014, **58**, 359–373.

7 (*a*) L. Prodi, F. Bolletta, M. Montalti and N. Zaccheroni, *Coord. Chem. Rev.*, 2000, **205**, 59–83; (*b*) H. Kobayashi, M. Ogawa, R. Alford, P. L. Choyke and Y. Urano, *Chem. Rev.*, 2010, **110**, 2620–2640; (*c*) L. Yuan, W. Lin, K. Zheng, L. He and W. Huang, *Chem. Soc. Rev.*, 2013, **42**, 622–661; (*d*) Z. Guo, S. Park, J. Yoon and I. Shin, *Chem. Soc. Rev.*, 2014, **43**, 16–29; (*e*) Y. Yang, Q. Zhao, W. Feng and F. Li, *Chem. Rev.*, 2013, **113**, 192–270.

8 (*a*) X.-F. Yang, X.-Q. Guo and Y.-B. Zhao, *Talanta*, 2002, **57**, 883–890; (*b*) T. Ueno, Y. Urano, H. Kojima and T. Nagano, *J. Am. Chem. Soc.*, 2006, **128**, 10640–10641; (*c*) D. Yang, H. Wang, Z. Sun, N.-W. Chung and J. Shen, *J. Am. Chem. Soc.*, 2006, **128**, 6004–6005; (*d*) P. Panizzi, M. Nahrendorf, M. Wildgruber, P. Waterman, J.-L. Figueiredo, E. Aikawa, J. McCarthy, R. Weissleder and S. A. Hilderbr and, *J. Am. Chem. Soc.*, 2009, **131**, 15739–15744; (*e*) D. Oushiki, H. Kojima, T. Terai, M. Arita, K. Hanaoka, Y. Urano and T. Nagano, *J. Am. Chem. Soc.*, 2010, **132**, 2795–2801; (*f*) C. Song, Z. Ye, G. Wang, J. Yuan and Y. Guan, *Chem. – Eur. J.*, 2010, **16**, 6464–6472; (*g*) K. Xu, H. Chen, J. Tian, B. Ding, Y. Xie, M. Qiang and B. Tang, *Chem. Commun.*, 2011, **47**, 9468–9470; (*h*) J. Tian, H. Chen, L. Zhuo, Y. Xie, N. Li and B. Tang, *Chem. – Eur. J.*, 2011, **17**, 6626–6634; (*i*) Y. Koide, M. Kawaguchi, Y. Urano, K. Hanaoka, T. Komatsu, M. Abo, T. Terai and T. Nagano, *Chem. Commun.*, 2012, **48**, 3091–3093; (*j*) Q. Zhang, Z. Zhu, Y. Zheng, J. Cheng, N. Zhang, Y.-T. Long, J. Zheng, X. Qian and Y. Yang, *J. Am. Chem. Soc.*, 2012, **134**, 18479–18482; (*k*) A. J. Shuhendler, K. Pu, L. Cui, J. P. Uetrecht and J. Rao, *Nat. Biotechnol.*, 2014, **32**, 373–382.

9 (*a*) Z. Sun, H. Wang, F. Liu, Y. Chen, P. K. H. Tam and D. Yang, *Org. Lett.*, 2009, **11**, 1887–1890; (*b*) T. Peng and D. Yang, *Org. Lett.*, 2010, **12**, 4932–4935; (*c*) F. Yu, P. Li, G. Zhao, T. Chu and K. Han, *J. Am. Chem. Soc.*, 2011, **133**, 11030–11033; (*d*) F. Yu, P. Song, P. Li, B. Wang and K. Han, *Analyst*, 2012, **137**, 3740–3749; (*e*) K.-K. Lin, S.-C. Wu, K.-M. Hsu, C.-H. Hung, W.-F. Liaw and Y.-M. Wang, *Org. Lett.*, 2013, **15**, 4242–4245; (*f*) F. Yu, P. Li, B. Wang and K. Han, *J. Am. Chem. Soc.*, 2013, **135**, 7674–7680; (*g*) B. Wang, F. Yu, P. Li, X. Sun and K. Han, *Dyes Pigm.*, 2013, **96**, 383–390; (*h*) X. Sun, Q. Xu, G. Kim, S. E. Flower, J. P. Lowe, J. Yoon, J. S. Fossey, X. H. Qian, S. Bull and T. D. James, *Chem. Sci.*, 2014, DOI: 10.1039/C4SC01417K.

10 (*a*) A. Helal, M. H. Or Rashid, C.-H. Choi and H.-S. Kim, *Tetrahedron*, 2011, **67**, 2794–2802; (*b*) L. Yuan, W. Lin, J. Song and Y. Yang, *Chem. Commun.*, 2011, **47**, 12691–12693; (*c*) J.-T. Hou, K. Li, K.-K. Yu, M.-Z. Ao, X. Wang and X.-Q. Yu, *Analyst*, 2013, **138**, 6632–6638; (*d*) J.-T. Hou, K. Li, B.-Y. Liu, Y.-X. Liao and X.-Q. Yu, *Tetrahedron*, 2013, **69**, 2118–2123.

11 (*a*) G.-J. Zhao, J.-Y. Liu, L.-C. Zhou and K.-L. Han, *J. Phys. Chem. B*, 2007, **111**, 8940–8945; (*b*) G.-J. Zhao and K.-L. Han, *Acc. Chem. Res.*, 2012, **45**, 404–413.

12 T. Guo, L. Cui, J. Shen, R. Wang, W. Zhu, Y. Xu and X. Qian, *Chem. Commun.*, 2013, **49**, 1862–1864.

13 T. Salonen, O. Sareila, U. Jalonen, H. Kankaanranta, R. Tuominen and E. Moilanen, *Br. J. Pharmacol.*, 2006, **147**, 790–799.

